

## Selectivity A Study of the effect of pH of the Zn substituent ions on the structural and magnetic properties of copper-ferrite complex

Zainab .T. S. and Fares A. Yasseen

Department of Physics, Faculty of Science, University of Kufa, Al-Najaf, Iraq

\*Corresponding Author E-mail: [zainabt.alkhikani@student.uokufa.edu.iq](mailto:zainabt.alkhikani@student.uokufa.edu.iq)  
[Fares.alkufy@uokufa.edu.iq](mailto:Fares.alkufy@uokufa.edu.iq)

### ARTICLE INF.

#### Article history:

Received: 28 MAR., 2025

Revised: 8 APR., 2025

Accepted: 18 APR., 2025

Available Online: 28 JUN. 2025

#### Keywords :

sol-gel combustion,  
copper-zinc spinel  
ferrites,  
magnetic properties  
(VSM)

### ABSTRACT

Copper-zinc ferrite composites with composition  $(Cu_{1-x}Zn_xFe_2O_4)$  at  $x = 0.75$  were successfully prepared using the sol-gel method. The effect of varying pH (pH = 7–11) on the structural and magnetic properties was studied. X-ray diffraction (XRD) results showed that all samples possessed a single-phase cubic spinel crystalline phase, which was confirmed by FTIR analysis, which revealed the presence of distinct M–O bonds at the tetrahedral and octahedral sites with absorption peaks observed in the frequency range of  $490–535\text{ cm}^{-1}$ . FE-SEM images showed the presence of nearly regular nanocrystals, with particle size variation associated with pH variation. EDS results confirmed the purity of the samples and their absence of impurities. Magnetic tests using VSM showed that all samples possessed soft ferrite properties, with saturated magnetism (Ms) ranging between 13.40 and 17.40 emu/g, indicating their potential for use in electronic and micromagnetic applications.

DOI: <https://doi.org/10.31257/2018/JKP/2025/v17.i01.19129>

## دراسة تأثير الرقم الهيدروجيني لأيونات الزنك البديلة على الخواص البنيوية والمغناطيسية لمركب النحاس-فرايت

زينب طالب شاكر فارس عبد ياسين

قسم الفيزياء، كلية العلوم، جامعة الكوفة، النجف، العراق

### الكلمات المفتاحية:

احتراق السول-جل،  
فيريتات السبينييل النحاسي -  
الزنك،

الخصائص المغناطيسية  
(VSM)

### الخلاصة

تم تحضير مركب فرايت النحاس والزنك حسب الصيغة  $(Cu_{1-x}Zn_xFe_2O_4)$  بنجاح وباستخدام طريقة السول-جل عند  $x = 0.75$ . دُرست آثار تغير الرقم الهيدروجيني من (pH = 7-11) على الخواص البنيوية والمغناطيسية. وأظهرت نتائج حيود الأشعة السينية (XRD) أن جميع العينات تمتلك طورًا بلوريًا أحادي الطور من

السبينيل المكعب، وهو ما تم تأكيده من خلال تحليل FTIR، الذي كشف عن وجود روابط M–O مميزة في المواقع رباعية السطوح وثمانية السطوح، مع قمم امتصاص لوحظت في نطاق ترددي يتراوح بين (490- 535) سم<sup>-1</sup>. وأظهرت صور المجهر الإلكتروني الماسح FE-SEM وجود بلورات نانوية شبه منتظمة، مع اختلاف في حجم الجسيمات يرتبط بتغير الرقم الهيدروجيني. وأكدت نتائج EDS نقاء العينات وخلوها من الشوائب. كما أظهرت الاختبارات المغناطيسية باستخدام VSM أن جميع العينات تمتلك خصائص الفريت الناعمة، مع مغناطيسية مشبعة (Ms) تتراوح بين 13.40 و 17.40 emu / g، مما يشير إلى إمكاناتها للاستخدام في التطبيقات الإلكترونية والمغناطيسية الدقيقة.

## 1. INTRODUCTION

Magnetic nanoparticles (MNPs) are widely used in business and medical fields for their distinct chemical, thermal, and magnetic capabilities. They can be utilized as catalysts or magnetic data storage materials [1,2]. Ferro-magnetic materials have a unique super paramagnetic feature that makes them useful in biomedicine, drug delivery, and cancer treatment[3]. Ferrites are a type of magnetic ceramic substance commonly utilized in the microwave and electrical sectors. They have excellent electrical resistance and advantageous ferromagnetic properties[4]. Ferrites are classified into two categories based on their magnetic properties: hard and soft. This classification is based on ferrite's capacity to magnetize or demagnetize itself. Soft ferrites are easily magnetized or demagnetized, but hard ferrites are difficult to magnetize or demagnetize[5]. The ferrites are classified into three types according on their chemical composition [6]: Garnet and hexagonal, and spinel. Because of its strong magnetic characteristics and wide range of applications, we shall focus our research on the latter. Spinel ferrites have strong magnetic and electrical capabilities due to the distribution of positive ions (cations)

between tetrahedral and octahedral sites[7].

According to the crystal structure, zinc ferrite is normal spinel and copper ferrite is an inverse spinel ferrite[8]. When zinc is substituted for copper ferrite, the dielectric characteristics of copper ferrite are altered, which is advantageous in a variety of device applications. Cu-Zn nanoferrite is an important ferrite material because of its strong dielectric and electrical resistance[9]. Therefore, it is important to study their magnetic properties [10,11].

## 2. Experimental Part.

Cu-Zn ferrites of composition  $(Cu_{1-x}Zn_xFe_2O_4)$  (where;  $x=0.75$ ) were synthesized using auto-combustion sol-gel method. The appropriate amount of nitrates [ $Zn(NO_3)_2 \cdot 6H_2O$ ,  $Cu(NO_3)_2 \cdot 3H_2O$  and  $Fe(NO_3)_3 \cdot 9H_2O$  and citric acid [ $C_6H_8O_7 \cdot H_2O$ ] were dissolved in distilled water to form aqueous solution. Different pH values were used ((i.e. pH=7,8,9,10,11) using ammonia solution. Then the aqueous solution was heated and evaporated at 90°C under intensive stirring to transform into a highly viscous gel. The obtained gel is dried inside electric oven at a temperature of 120 °C. The pellet

samples were sintered at 1100°C for 3 hours.

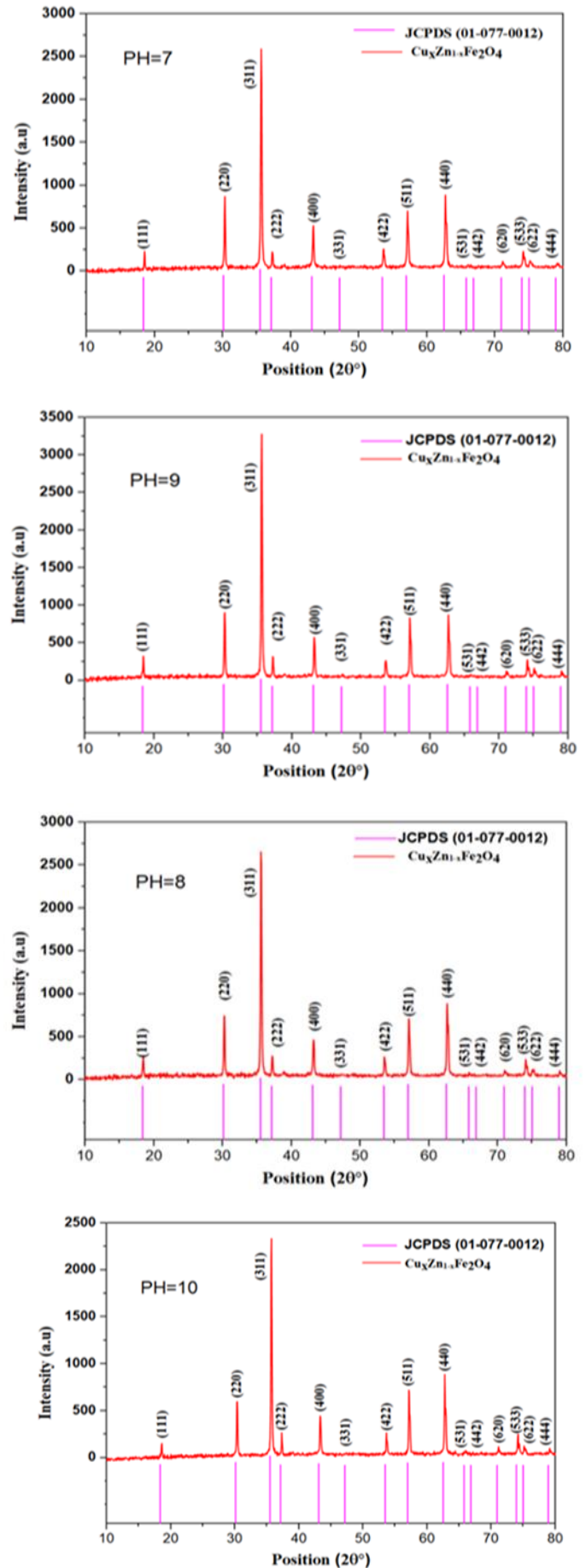
The presence of a distinct single-phase spinel ferrite structure is confirmed by the X-ray diffraction technique, which was used for phase identification and structural characterization (Target: Cu-K $\alpha$ , 10°-90°, step size: – 0.02° holding time: 0.2 seconds). Using FE- SEM machine, the SEM image of the ferrite powder produced was acquired. Magnetic properties such as coercivity, remanence, and saturation magnetization were measured using VSM.

### 3. Results and Discussion.

$Cu_{1-x}Zn_xFe_2O_4$  is the general formula for synthesized spinel ferrite. When compared to the typical XRD pattern of Cu-Zn spinel ferrite, the XRD spectra for  $x = 0.75$ , which are displayed in Figure(1), confirming the formation of single phase Cu-Zn spinel ferrite. When compared to single-phase cubic spinel, the most intense peaks in all samples were (220), (311), (222), (400), (422), (333), and (440). Using Debye Scherrer's formula, the average crystallite size for each sample was determined in relation to the high-intensity peak plane (311). The crystallite size(D) can be determined using Debye Scherrer's formula[12, 13]

$$D = \frac{0.9\lambda}{B \cos \theta_B}$$

where  $\lambda$  is the wavelength,  $\theta_B$  for Bragg's angle (in degrees), and  $B$  for the width of the main peak at FWHM (in radians).



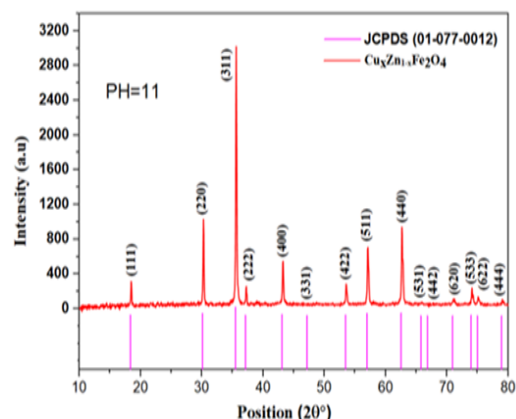


**Figure (1):** XRD pattern for Cu-Zn spinel ferrite synthesized

Table (1) shows the effect of pH variation on the structural parameters of Cu-Zn spinel ferrite at fixed Zn substitution ( $x = 0.75$ ). The observed slight variations in lattice parameters with pH may be attributed to changes

in crystallization conditions and microstructural distortions introduced during synthesis. However, the lattice parameter value drops for  $x = 0.75$ , this can be explained by the lattice distortion caused by the additional Zn addition in the Cu-Zn spinel ferrite[14]

**Table (1):** Structural parameters  $Cu_{1-x}Zn_xFe_2O_4$

Component	pH	(hkl)	Peak position (2 Theta)	FWHM	Crystallite size D(nm)	$\delta = 1/D^2$	$d_{hkl}(A^\circ)$	$a(A^\circ)$
$Cu_{1-x}Zn_xFe_2O_4$	7	(311)	35.679	0.197	42.385	0.00055	2.51651	8.353
	8	(311)	35.604	0.140	59.762	0.00028	2.52166	8.371
	9	(311)	35.622	0.197	42.385	0.00055	2.52039	8.367
	10	(311)	35.722	0.197	42.385	0.00055	2.51358	8.343
	11	(311)	35.632	0.197	42.385	0.00055	2.51974	8.363

Figure(2)demonstates the FE-SEM of copper ferrite doped with zinc. Nano-crystals were found for each of the prepared compounds. The particles differ from each other in size as it was noticed that the size changes with the change in pH with the replacement of Cu ions by Zn ions in the crystal lattice because the radius of Cu ions is less than Zn ions[15]. This change ranges between (20.22 – 38.10 ) nm. It was also observed that

particles accumulated for all prepared samples with different sizes, which are nano-sized, and these results were consistent with the results of the XRD examination.

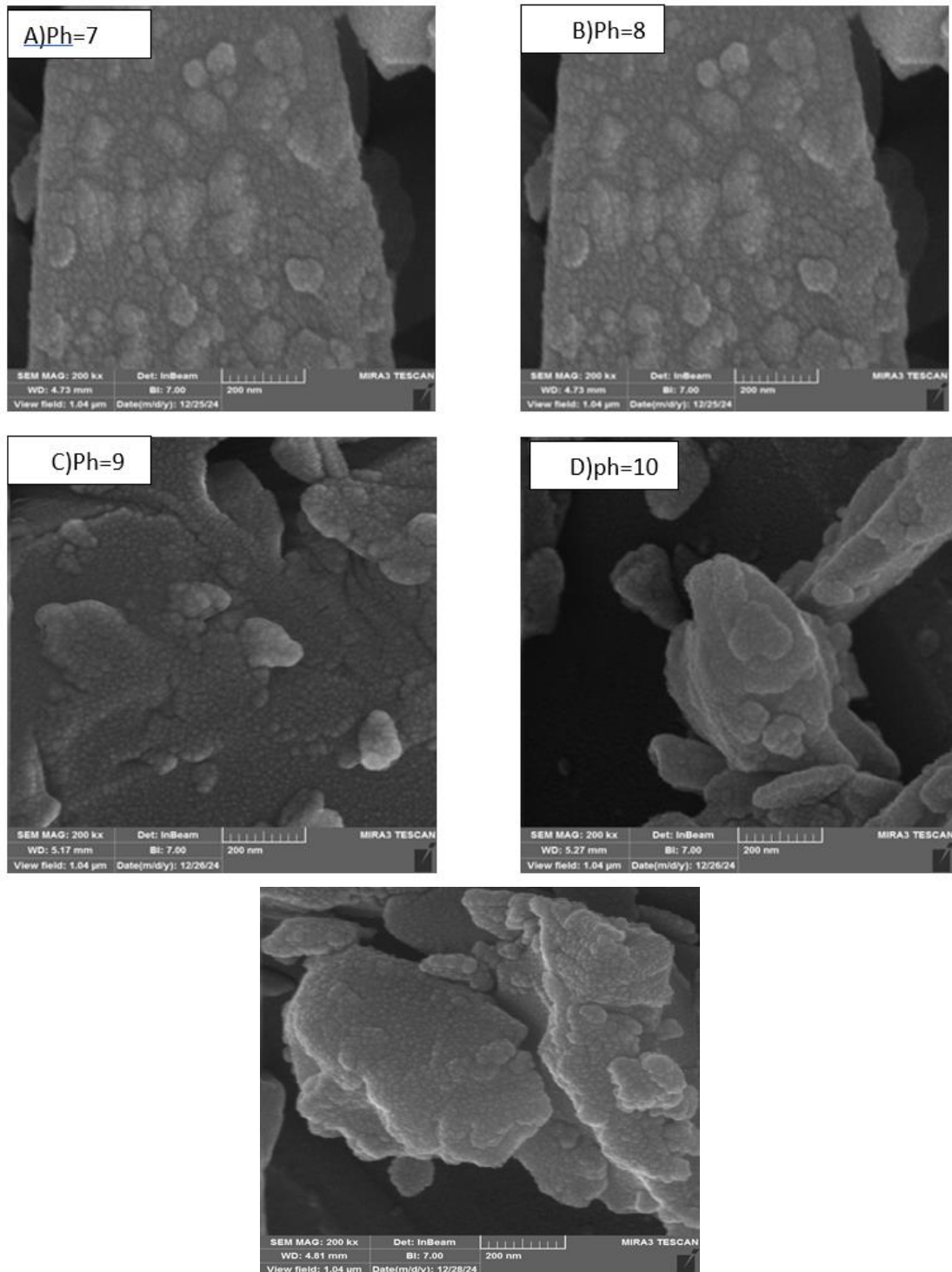


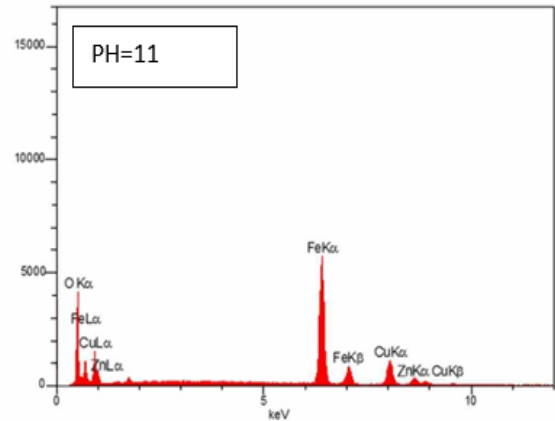
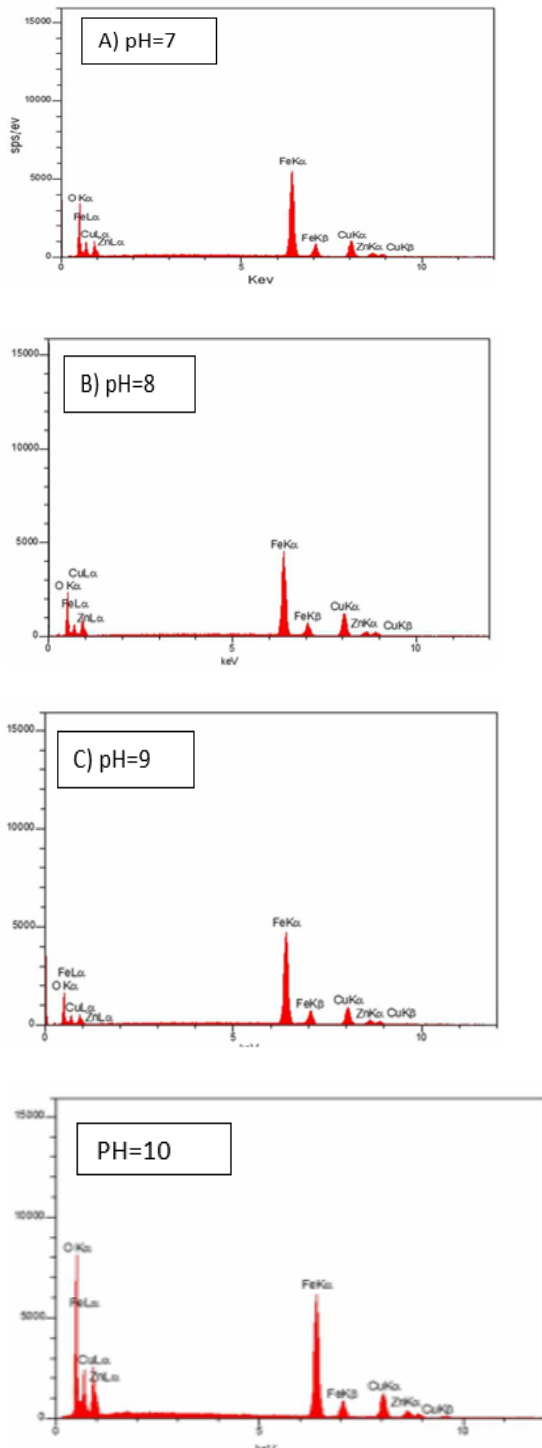
**Figure (3):** FE-SEM images of  $(Cu_{1-x}Zn_xFe_2O_4)$

EDS analysis was used to identify the chemical elements of the prepared ferrite compounds [16].

This analysis (EDS) showed the effect of the pH added to the ferrite compound as a result of stimulating the

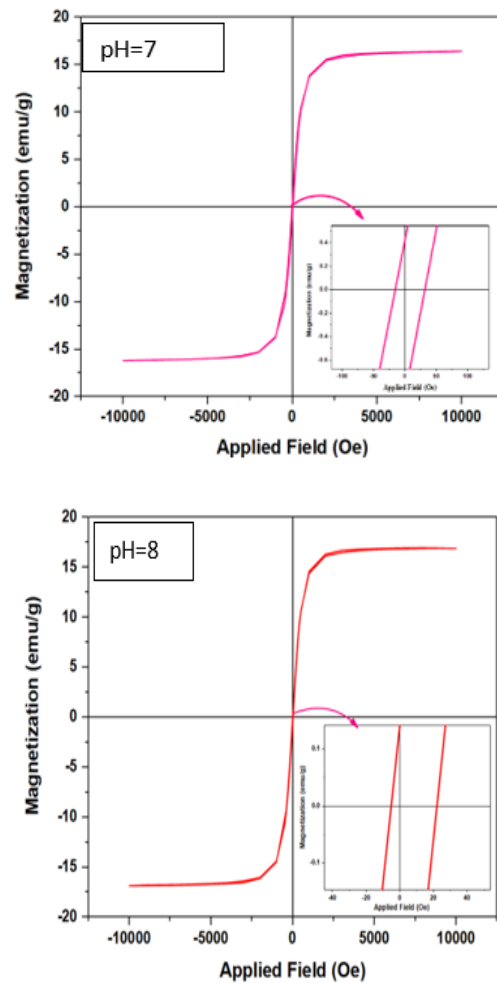
electrons to move. Figure (4) showed that the elements that make up the ferrite compound consist of iron, oxygen, zinc and copper according to the proportions shown in the Figure (4). The atomic ratios fall within the experimental error and the absence of

impurities was noted. This indicates the purity of the samples and there is no loss or increase in the number of elements of the ferrite compound, which indicates the success of the preparation method. This also agrees completely with the results of XRD.



**Figure (4):** EDS for ferrite component  $Cu_{1-x}Zn_xFe_2O_4$

The saturation magnetization ( $M_s$ ) and coercivity ( $H_c$ ) of Nano powders synthesized by the sol-gel method are shown in Figure (5).



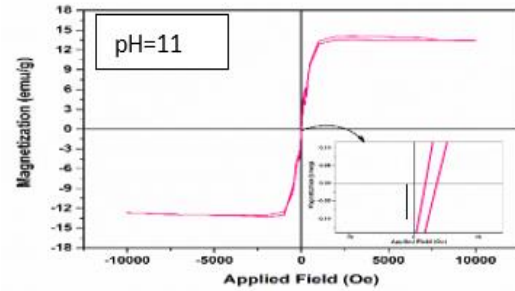
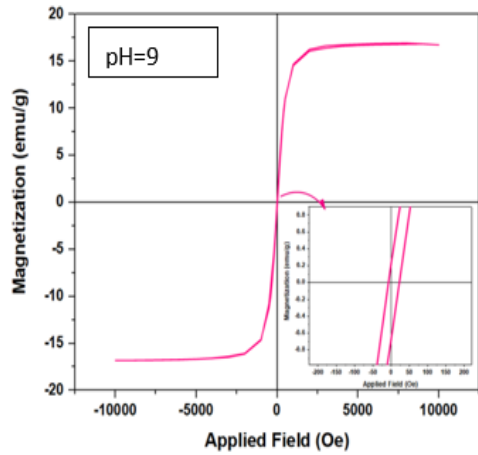


**Figure (5):** Hysteresis loop for Cu-Zn spinel ferrite synthesized

The obtained results of  $M_s, M_r, H_c, R$  and  $k$  are presented in Table (2).

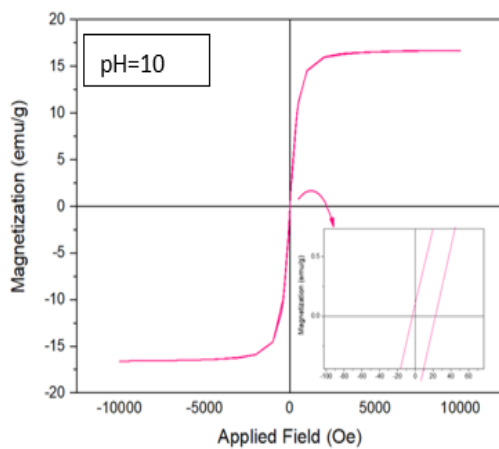


**Table (2):** Magnetic Saturation ( $M_s$ ), Remaining Magnetism ( $M_r$ ) and force Coercive ( $H_c$ ) as a function of Copper with deferent pH.

Component	pH	$M_s(\text{emu/g})$	$M_r(\text{emu/g})$	$H_c \text{ Oe} = \frac{-H_c + H_c}{2}$	$R = M_r/M_s$	$k = \frac{(M_s * H_c)}{0.96} (\text{erg/g})$
$\text{Cu}_{1-x}\text{Zn}_x\text{Fe}_2$	pH=7	17.40913	0.412624	9.350284	0.025146001	159.823
	pH=8	16.88126	0.14036	8.496248	0.008314545	149.4035
	pH=9	16.73558	0.210691	8.187503	0.012589405	142.7319
	pH=10	16.70722	0.10777	10.03636	0.006450505	174.6663
	pH=11	13.40126	-0.18107	5.425178	-0.013511416	75.73356

Where,  $k$  it is called the anisotropy constant, it can be seen that the larger this number of the  $k$  is, the more magnetism aligns and takes the direction of the magnetic field. This means that this material can be magnetized because its ions or molecules align with the electric field in one direction, and the  $M_s$  is highest

when  $\text{pH}=7$  due to the high magnetic anisotropy  $k$  and the particle shape of the secondary particles, as most of the particles align in one direction. This alignment leads to the particle diameter being smaller. In addition, the deceleration ring is narrower. In fact, this narrowing of the ring can affect the

particle size and surface shape, and thus affect the values of  $M_s$  and  $H_c$ .

$R$  is the ratio between  $M_R$  and  $M_S$ . The closer this ratio is to one, the better it is. This means that the hysteresis loop is vertical, i.e. there is no tilt in it. If its value is equal to one, this means that there is no loss in the molecule. To illustrate, the particles have a rapid response to the magnetic field, which means that it is ideal. On the other hand, the coercive field ( $H_c$ ) was calculated by averaging the values between the negative and positive field axes where the magnetization of the hysteresis loop is zero (i.e. when  $y=0$ , and it was found to range between  $H_c$  9.35 and 5.425). The negative value of remanent magnetization ( $M_r$ ) at  $pH = 11$  may be attributed to magnetic relaxation or antiparallel alignment of magnetic domains, likely induced by structural distortions or surface anisotropy under high  $pH$  synthesis conditions. The sharp drop in  $M_r$  from  $pH = 7$  to  $pH = 8$  may be related to increased particle size or agglomeration effects, which reduce the remanent magnetization due to loss of magnetic ordering.

One of the best methods for identifying the structural composition of various materials is FT-IR spectroscopy[17]. The two sublattices of cubic spinel ferrites were octahedral (B) and tetrahedral (A). There are typically two absorption bands in the 400–600  $cm^{-1}$  range that correspond to these sites[18]. The stretching vibration mode of metal-oxygen in the tetrahedral sites is responsible for the higher frequency absorption band ( $\nu_1$ ), while the stretching vibrations of octahedral group complexes are responsible for the

lower frequency absorption band ( $\nu_2$ )[19]. Figure (6) shows the FTIR spectrum of the ferrite compound at  $x=0.75$  in the frequency range (400-4000)  $cm^{-1}$  where there are several bonds located between (535- and 490)  $cm^{-1}$  through the vibration sites. The structural changes resulting from the metal ions that strongly affected the lattice vibrations and these vibrations also depend on the cations, oxygen ions, and the strength of the bonding, It is due to stretching vibrations in the tetrahedral sites (A-sites) between the metal and oxygen ions, The lower frequency is attributed to stretching vibrations at the octahedral sites (B-sites). The shapes indicate a distinctive feature for all ferrites, as the vibration modes are consistent with all spinel compounds that confirmed the formation of metal oxides for the prepared compounds. The main vibrations occur between the tetrahedral (800-600)  $cm^{-1}$  and octahedral (600-400) $cm^{-1}$  sites. As a result of these vibrations, a small shift at the peaks occurs when we replace the Cu ion by the Zn ion because the radii of Cu are less than the radii of Zn. The metal ions affect the lattice and it consists of two bands. This decrease is due to the iron and oxygen ions in the octahedral and tetrahedral groups.(i.e A change in the binding energy within the crystal lattice occurs, leading to a slight shift of the peaks in the FTIR spectrum and this change is due to the effect of  $Zn^{+2}$  on the rigidity of the M–O bonds, which in turn affects the vibration pattern[20].

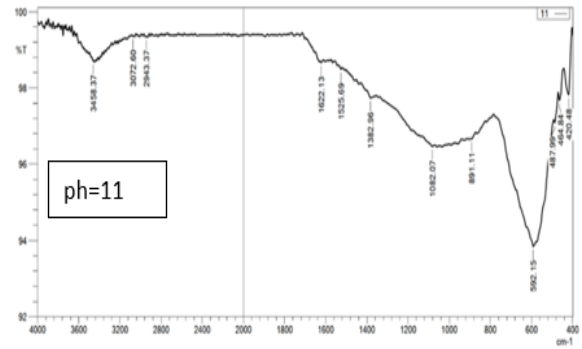
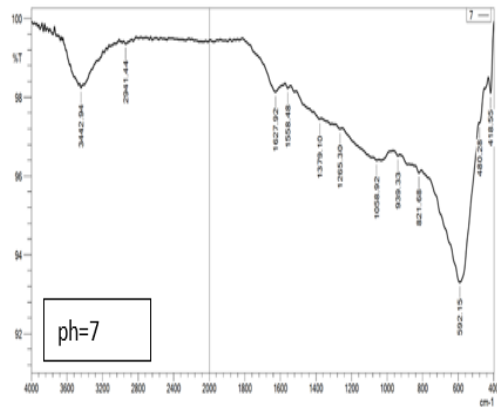
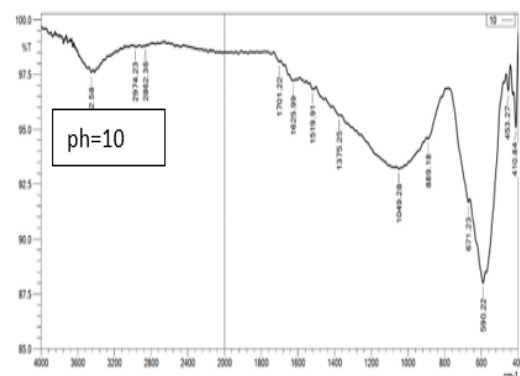
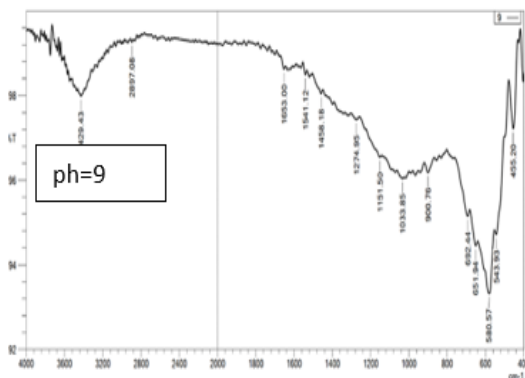
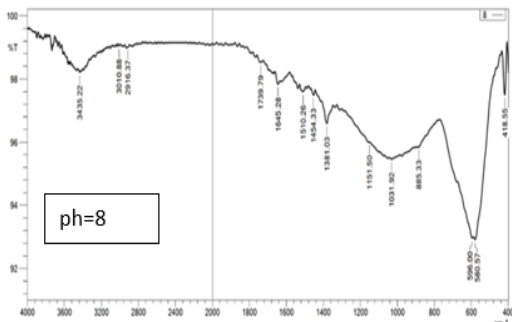


Figure (6): FT-IR spectra



#### 4. Conclusions.

Copper zinc ferrite compound with chemical formula  $(Cu_{1-x}Zn_xFe_2O_4)$  at  $(X=0.75)$  ratio was successfully prepared by sol joule method and the effect of pH was studied and characterized using  $(PH=7,8,9,10,11)$  where it was observed that all samples contain a single-phase cubic spinel ferrite structure through (XRD) which is consistent with (FTIR). Scanning electron microscopy (FE-SEM) identified nanocrystals and a somewhat uniform distribution of particles. Analysis (EDS) revealed the absence of impurities, which indicates the purity of the samples and there is no loss or increase in the number of elements of the ferrite compound at any percentage of pH, which indicates the success of the preparation method. This is also completely consistent with the results of XRD. The study of the magnetic properties (VSM) confirmed the presence of soft spinel ferrite, where the saturated magnetism ranged between  $(13.40-17.40)$  emu/g, which confirms that soft spinel ferrite was obtained.

#### References.

- [1] Wei, J., Xu, H., Sun, Y., Liu, Y., Yan, R., Chen, Y., & Zhang, Z. (2024). Magnetite Nanoparticle Assemblies and Their Biological Applications: A Review. *Molecules*, 29(17), 4160.
- [2] Zhang, J., Liu, H., Wang, J., Shang, J., Xu, M., Zhu, X., ... & Zhao, X. (2024). Bioinspired Hollow Mesoporous Silica Nanoparticles Coating on Titanium Alloy with Hierarchical Structure for Modulating Cellular Functions. *Journal of Bionic Engineering*, 21(3), 1427-1441.
- [3] Zargar, T. and A. Kermanpur, *Effects of hydrothermal process parameters on the physical, magnetic and thermal properties of Zn<sub>0.3</sub>Fe<sub>2.7</sub>O<sub>4</sub> nanoparticles for magnetic hyperthermia applications*. *Ceramics International*, 2017. 43(7): p. 5794-5804.
- [4] Ghasemi, A. and M. Mousavinia, *Structural and magnetic evaluation of substituted NiZnFe<sub>2</sub>O<sub>4</sub> particles synthesized by conventional sol–gel method*. *Ceramics International*, 2014. 40(2): p. 2825-2834.
- [5] AL-Kufy, F.A.Y.H., *Characterization of Nano Spinel Ferrite Fields*, 2020, College of Science, University of Babylon.
- [6] Gupta, M., et al. (2023). Advances in spinel ferrite nanoparticles for biomedical and electronic applications. *Journal of Magnetism and Magnetic Materials*, 570, 170512.
- [7] Muthana, E. A., *Structural, Electrical and magnetic properties of superparamagnetic TiO<sub>2</sub> mixed Zn<sub>x</sub>Mn<sub>1-x</sub>Fe<sub>2</sub>O<sub>4</sub> Nanoferrites*. 2022.
- [8] Kumar, R., et al. (2023). Structural and magnetic studies of inverse spinel CuFe<sub>2</sub>O<sub>4</sub> ferrite: Influence of cation distribution. *Ceramics International*, 49(8), 12231-12245.
- [9] Ridha, S.M.A., *X-ray studies and electrical properties of the zinc-substituted copper nanoferrite synthesized by sol-gel method*. *Int. J. Compos. Mater.*, 2015. 5(6): p. 195-201.
- [10] Singh, R., & Thakur, P. (2023). Structural and magnetic behavior of Zn-substituted copper ferrites synthesized via sol–gel route. *\*Journal of Alloys and Compounds\**, 934, 167976.
- [11] Patel, M., & Sahoo, B. (2023). A review on spinel ferrite nanoparticles for magnetic applications. *\*Materials Today: Proceedings\**, 86, 1168-1176.
- [12] Nigam, A. and S. Pawar, *Structural, magnetic, and antimicrobial properties of zinc doped magnesium ferrite for drug delivery applications*. *Ceramics International*, 2020. 46(4): p. 4058-4064.
- [13] Nigam, A. and S. Pawar, *Synthesis and characterization of ZnO nanoparticles to optimize drug loading and*

- release profile for drug delivery applications*. *Materials Today: Proceedings*, 2020. 26: p. 2625-2628.
- [14] Parashar, J., et al., *Dielectric behaviour of Zn substituted Cu nano-ferrites*. *Journal of Magnetism and Magnetic Materials*, 2015. 394: p. 105-110.
- [15] Sharma, R., et al. (2023). *EDS and XRD analysis of Cu-Zn ferrite nanoparticles: Effect of synthesis conditions on structural properties*. *Journal of Magnetism and Magnetic Materials*, 570, 170659.
- [16] Rais, A., et al., *Copper substitution effect on the structural properties of nickel ferrites*. *Ceramics International*, 2014. 40(9): p. 14413-14419.
- [17] Gupta, P., et al. (2022). *Fourier transform infrared spectroscopy (FT-IR) study of Cu-Zn ferrites: Effect of composition on vibrational frequencies*. *Materials Chemistry and Physics*, 287, 126841.
- [18] Bouhadouza, N., et al., *Structural and vibrational studies of  $NiAl_xFe_{2-x}O_4$  ferrites ( $0 \leq x \leq 1$ )*. *Ceramics international*, 2015. 41(9): p. 11687-11692.
- [19] Khan, I., et al. (2024). *Effect of pH on structural, morphological, and magnetic properties of sol-gel synthesized ferrite nanoparticles*. *Ceramics International*, 50(1), 894-905.
- [20] Iqbal, M. J., & Ashiq, M. N. (2022). *FTIR and magnetic characterization of copper zinc ferrite nanomaterials*. *Materials Chemistry and Physics*, 285, 126145.